Journal of Applied Physics ARTICLE scitation.org/journal/jap

On the mechanism underlying the elimination of nitrogen-oxygen shallow thermal donors in nitrogen-doped Czochralski silicon at elevated temperatures

Cite as: J. Appl. Phys. **129**, 145702 (2021); doi: 10.1063/5.0045680
Submitted: 28 January 2021 · Accepted: 26 March 2021 ·
Published Online: 12 April 2021

Tong Zhao,[1] Chenqiang Hua,[2] Wu Lan,[1] Yuxin Sun,[1] Defan Wu,[1] Yunhao Lu,[2] Xiangyang Ma,[1,a)] and Deren Yang[1,a)]

AFFILIATIONS

[1]State Key Laboratory of Silicon Materials and School of Materials Science and Engineering, Zhejiang University, Hangzhou 310027, China
[2]Department of Physics, Zhejiang University, Hangzhou 310027, China

[a)]**Authors to whom correspondence should be addressed:** mxyoung@zju.edu.cn and mseyang@zju.edu.cn

ABSTRACT

Nitrogen-doped Czochralski (NCZ) silicon has been a base material for integrated circuits. The interaction between nitrogen (N) and interstitial oxygen (O_i) atoms in the low temperature regime (300–650 °C), which leads to N–O complexes in the form of NO_x ($x = 1$, 2, or 3), forms a series of shallow thermal donors (denoted as N–O STDs). Such N–O STDs are detrimental to the stability of electrical resistivity of NCZ silicon. In this work, we have experimentally investigated the elimination of N–O STDs in NCZ silicon by means of conventional furnace anneal (CFA) and rapid thermal anneal at elevated temperatures ranging from 900 to 1250 °C, aiming to explore the underlying mechanism. It is found that most of the N–O STDs formed in NCZ silicon can be eliminated by a very short period of anneal at the aforementioned temperatures, providing solid evidence for the viewpoint that the elimination of N–O STDs is ascribed to the decomposition of NO_x complexes. Somewhat unexpectedly, the residual N–O STDs are much more after the 1250 °C/2 h CFA than after the 900 °C/2 h or 1000 °C/2 h counterpart, which is found to be due to the fact that more nitrogen pairs [(N_2)s] are remaining after the 1250 °C/2 h CFA. It is proposed that most of the (N_2) atoms are involved in the growth of grown-in oxide precipitates during the 900 or 1000 °C/2 h CFA. The first-principles calculations and molecular dynamics simulation indicate that the elimination of N–O STDs is essentially ascribed to the destruction of "NO *ring*" that is the core of NO_x complexes. Furthermore, based on the experimental and theoretical results, we have made a thorough thermodynamic analysis to account for the details of elimination of N–O STDs as revealed in this work. It is believed that our experimental and theoretical studies have gained more insight into the N–O STDs in NCZ silicon.

I. INTRODUCTION

Nitrogen (N) doping in Czochralski (CZ) silicon has been well proved to exhibit prominent advantages in improving mechanical strength,[1,2] enhancing oxygen precipitation associated internal gettering and making it easier to annihilate voids.[3–9] Consequently, N-doped CZ (NCZ) silicon has been widely applied in manufacturing integrated circuits. In the past three decades, the interaction between N and interstitial oxygen (O_i) impurities in CZ silicon has been a subject matter of interest. It has been found that annealing NCZ silicon in the temperature range of 300–650 °C leads to generating a series of N–O complexes, which exhibit shallow thermal donor properties (denoted as N–O STDs hereafter), with ionization energies of 34–37 meV.[10–17] Voronkov *et al.* found that the concentration of N–O STDs is proportional to the square root of N concentration.[18] Considering that nitrogen pair/molecule (N_2) as a di-interstitial is the primary form of N in silicon at room temperature (RT) and will dissolve into two interstitial nitrogen (N_i) atoms at higher temperatures,[19–21] they concluded that there was only one N atom in an individual N–O STD. Wagner *et al.* and Alt *et al.*

intensively studied the relationship between the concentration of N–O STDs and that of O_i atoms, leading to the conclusion that an individual N–O STD contains 1–3 O_i atoms.[22,23] Combining with the result of Voronkov *et al.*, they pointed out that the N–O STDs could exist in the forms of NO, NO_2, and NO_3 complexes (denoted as NO_x when necessary, hereafter). As for the origin of N–O STDs, the theoretical studies based on first-principles calculations have provided quite a few insights. Gali *et al.* proposed that a so-called "NO *ring*," which is actually composed of two Si, one N_i, and one O_i atoms, acts as the core of N–O STDs.[24,25] Ewels *et al.* figured out the configuration of the NO_2 complex and substantially clarified the origin of its STD nature.[26] Furthermore, they pointed out that adding more O_i atoms nearby the "NO *ring*" in an appropriate way would result in an increasingly shallow level of the donor associated with a certain N–O complex.

Like the oxygen-related thermal donors, N–O STDs can be eliminated by annealing at certain temperatures. Yang *et al.* reported that during the anneal at 650 °C, the N–O STDs first formed in the early stage and then disappeared gradually along with the extension of annealing time up to dozens of hours, accompanied by continuous reduction of the (N_2) and O_i atoms.[27] Hence, they believed that the heterogeneous nucleation of oxide precipitates on the N–O STDs as the precursors proceeded during the prolonged anneal at 650 °C, enabling the N–O STDs to lose their electrical activity. When annealed at higher temperatures, the elimination of N–O STDs becomes much faster. For example, most of the N–O STDs can be eliminated by conventional furnace anneal (CFA) at 900 °C for 30 min or at 1000 °C for 10 min.[28,29] Nevertheless, the elimination of N–O STDs by the CFA at even higher temperatures above 1000 °C and that by rapid thermal anneal (RTA) at elevated temperatures have been hardly investigated. Moreover, the underlying mechanism for the elimination of N–O STDs at elevated temperatures has also not been explicitly elucidated. There are two possible pathways for the N–O STDs to lose the electrical activity during annealing at elevated temperatures. One is that more O_i atoms aggregate onto the NO_x complexes to form larger clusters or even precipitates. The other is that the NO_x complexes are decomposed at elevated temperatures. Hence, more evidence need to be sought for the exploration of the underlying mechanism.

In this work, we have experimentally investigated the elimination of N–O STDs by means of CFA and RTA at 900, 1000, or 1250 °C. In the aspect of theoretical study, we have revisited the origin of N–O STDs starting from first-principles calculations and molecular orbital theory. Moreover, we have attempted molecular dynamics (MD) simulation of the behavior of N–O STDs at an elevated temperature of 1300 K (~1027 °C). Based on the experimental and theoretical results achieved, we have unequivocally pointed out that the elimination of N–O STDs is ascribed to the decomposition of NO_x ($x = 1$–3) complexes. From this standpoint, we have understood the related details of the elimination of N–O STDs through thermodynamic analysis on the decomposition reaction of NO_x complexes.

II. EXPERIMENTAL DETAILS

One ⟨100⟩-oriented, double-side polished, lightly phosphorus-doped *n*-type NCZ silicon wafer with a diameter of 150 mm was used. In such a wafer, phosphorus and nitrogen concentrations were 2.60×10^{14} and 2.06×10^{15} cm^{-3}, respectively, measured by secondary ion mass spectroscopy. The O_i concentration was 7.60×10^{17} cm^{-3}, measured by Fourier transformation infrared (FTIR) spectroscopy using a calibration coefficient of 3.14×10^{17} cm^{-2}. The substitutional carbon concentration was below the detection limit (5.0×10^{15} cm^{-3}) of FTIR spectroscopy. A number of specimens with a size of 2.0×2.0 cm^2 were cleaved from the aforementioned wafer for different anneals by means of CFA and RTA. The change in carrier concentration for a specimen before and after certain an anneal was obtained from the difference in resistivities, which were measured by a four-point probe (FPP). Herein, the transformation from resistivity to carrier concentration was in compliance with ASTM F723-88. In order to investigate the evolution of N–O STDs or (N_2) atoms arisen from different anneals, certain annealed specimens were characterized by FTIR spectroscopy at RT or at low temperature (8 K). For the sake of description and for the easiness of understanding, the annealing schemes and characterizations for different specimens were illustrated in Fig. 1. It should be mentioned that all the anneals were performed in an argon (Ar) atmosphere.

III. THEORETICAL CALCULATIONS

The static density functional theory (DFT) calculations and MD simulation were both run in the VASP code.[30–32] The Perdew–Burke–Ernzerhof (PBE) exchange-correlation functional at the general gradient approximation (GGA) level was adopted.[33,34] For the static DFT calculations, three silicon supercells were constructed. Concretely, the first silicon supercell consists of 216 Si atoms and a NO_2 complex composed of one interstitial nitrogen (N_i) and two O_i atoms with a C_{2v} symmetry. The second silicon supercell consists of 64 Si atoms and the aforementioned NO_2 complex. The third supercell also consists of 64 Si atoms but with randomly distributed one N_i and two O_i atoms. Geometric optimization was performed on each supercell. The heat capacities at 0–1500 K for the second and third supercells mentioned above were calculated by using the Phonopy source package. Thereby, the change in heat capacity due to the decomposition of NO_x complexes was obtained. A Γ-centered sampling of the Brillouin zone and a plane wave basis set with a cutoff energy of 450 eV were employed. The structure was optimized until the force on each atom was less than 0.01 eV/Å, and the threshold of calculations for energy comparison was 1.0×10^{-5} eV. Moreover, the MD simulation of the optimized structure of the first supercell as mentioned above was performed. For the MD simulation, a $1 \times 1 \times 1$ Gamma-only k point sampling of the Brillouin zone and a plane wave basis set with a cutoff energy of 450 eV were employed. The NVT ensemble, where N, V, and T represent the number of atoms, volume, and temperature of a supercell, was applied. The temperature of supercell was set to be 1300 K. The step time and step number were 1.5 fs and 2000, respectively. Besides, the energy convergence criterion was 5.0×10^{-5} eV.

IV. RESULTS AND DISCUSSION

A. Elimination of N–O STDs

Figure 2(a) shows the decrease in carrier concentration in the specimen along with the time of 900, 1000, or 1250 °C CFA following the pre-anneal at 650 °C for 2 h. It has been well known that

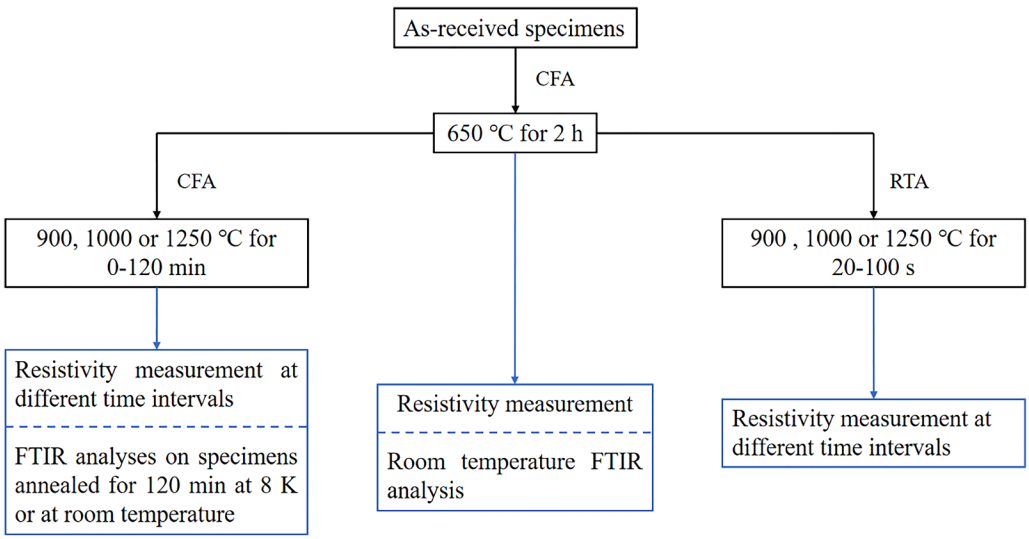

FIG. 1. Flow chart for the anneals and characterizations performed on different specimens.

the oxygen-related thermal donors can be substantially annihilated by the anneal at 650 °C for 30 min and, moreover, the N–O STDs can be sufficiently generated by the anneal at 650 °C for 2 h.[27] Therefore, after the pre-anneal at 650 °C for 2 h, the redundant donors besides the phosphorus atoms in the specimen are almost the N–O STDs. Previously, the N–O STDs were found to be eliminated by the anneal at 900 or 1000 °C.[28] Then, the decrease in carrier concentration as shown in Fig. 2(a) is ascribed to the gradual elimination of N–O STDs by the subsequent anneal at 900, 1000, or 1250 °C. As can be seen from Fig. 2(a), the carrier concentration decreases dramatically in the first 5 min anneal at each temperature. This indicates that most of the N–O STDs can be eliminated by such a short period of anneal. With the extension of annealing time, the carrier concentration in the specimen annealed at 1250 °C hardly changes, resulting from the nearly unchanged concentration of N–O STDs, while that in the specimen annealed at 900 or 1000 °C continues to decrease due to the successive elimination of N–O STDs. By comparison, the carrier concentration and, therefore, the N–O STD concentration in the specimen annealed at 1000 °C decreases more significantly. As seen, the terminal carrier concentration in the specimen annealed at 1000 °C for 120 min (2 h) is close to 2.60×10^{14} cm^{-3} that is nearly equivalent to the phosphorus concentration in the specimen, indicating that the N–O STDs were totally eliminated. Somewhat unexpectedly, the carrier concentration in the specimen subjected to the subsequent anneal at 1250 °C for 2 h is much higher than that in the specimen subjected to the subsequent anneal at 900 or 1000 °C for 2 h, which can only be understood through the thermodynamic analysis of the elimination of N–O STDs, as will be elucidated later.

Figure 2(b) shows the 8 K far-infrared FTIR spectra for those specimens of Fig. 2(a), which were subjected to the subsequent anneal at 900, 1000, and 1250 °C for 2 h. The absorption peaks at 240.4, 242.5, and 249.8 cm^{-1} are well documented to be corresponding to the N–O STDs in the forms of N–O-3 (NO_2), N–O-4 (NO), and N–O-5 (NO), respectively.[23] Apparently, the aforementioned absorption peaks emerging in Fig. 2(b) are originated from the residual N–O STDs after the 2 h anneal at 900, 1000, or 1250 °C. As can be derived, the concentration of residual N–O STDs in the specimen annealed at 1250 °C is the highest, while there are almost no residual N–O STDs in the specimen annealed at 1000 °C and that in the specimen annealed at 900 °C lies in between. Evidently, the result revealed in Fig. 2(b) is consistent with that shown in Fig. 2(a).

Figure 3 illustrates the RT middle-infrared FTIR spectra for those specimens of Fig. 2(a), which received the anneal at 900, 1000, and 1250 °C for 2 h following the 650 °C/2 h anneal. As a reference, the FTIR spectrum for the specimen only subjected to the 650 °C/2 h anneal is also included in Fig. 3. It is well known that the absorption peak at 963 cm^{-1} is ascribed to (N_2) atoms in silicon.[19] As can be seen from Fig. 3, the intensity of the absorption peak at 963 cm^{-1} of the specimen only subjected to the 650 °C/2 h anneal is the highest and that of the specimen with the subsequent 1250 °C/2 h anneal maintains almost the same. Moreover, the 963 cm^{-1} absorption peak is nearly indiscernible in the spectrum of the specimen with the subsequent 1000 °C/2 h anneal, while that can be distinguished from the spectrum of the specimen with the subsequent 900 °C/2 h anneal despite the significantly reduced intensity. Then, why the amounts of remaining of (N_2) atoms are so remarkably different after the anneal at different temperatures as mentioned above? Kvit *et al.* once reported that nitrogen impurities would aggregate at the interfaces between the oxide precipitates and silicon host in NCZ silicon.[35] Similarly, Adam *et al.* found that the implanted nitrogen atoms segregated at silicon/silicon oxide interface after certain anneal.[36,37] As it is well known, there should be grown-in oxide precipitates that are generated during the cooling process of crystal growth in NCZ silicon wafer.[3] When

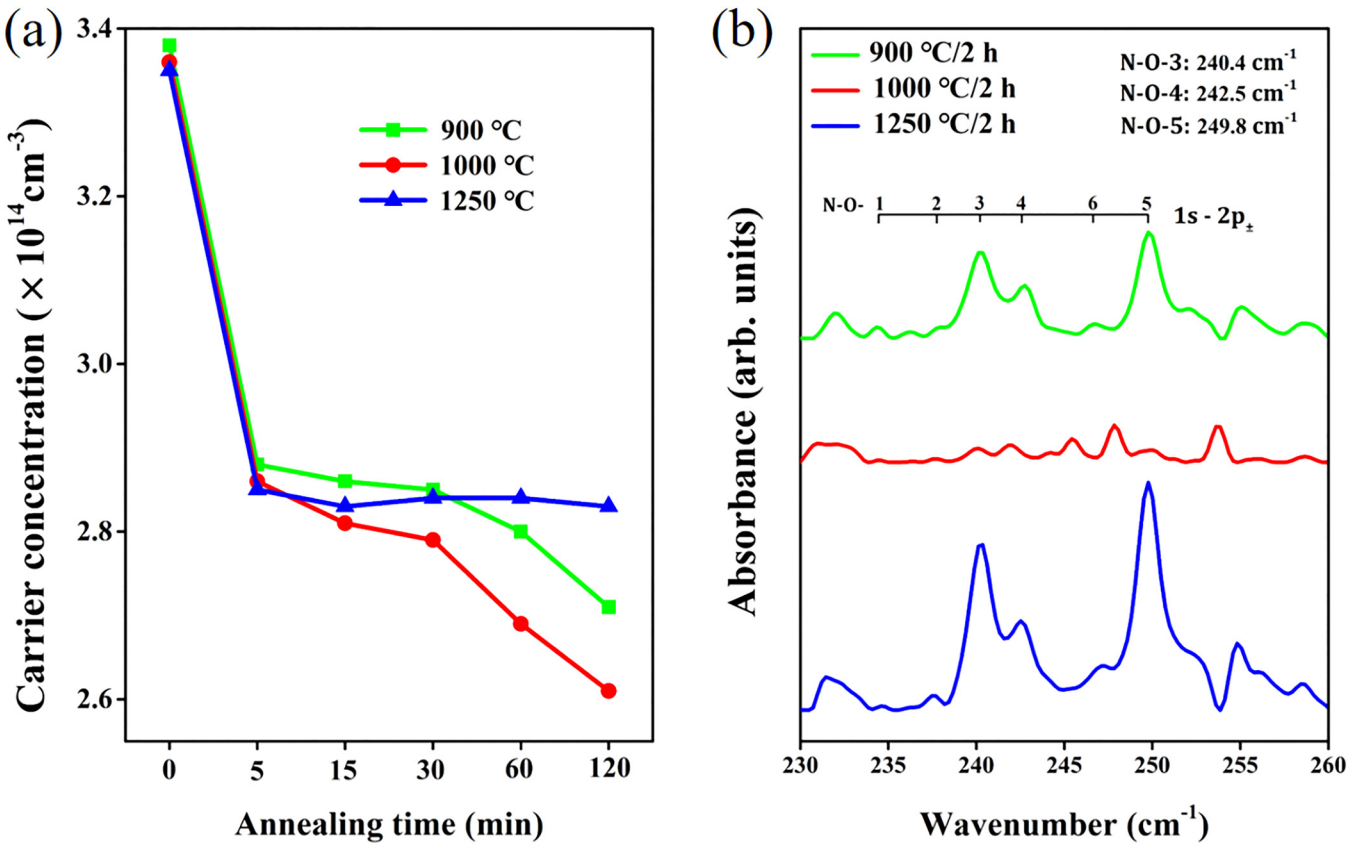

FIG. 2. (a) Decrease in carrier concentration in the specimen due to the CFA at 900, 1000, or 1250 °C for up to 120 min (2 h) after the 650 °C/2 h anneal. (b) 8 K far-infrared FTIR spectra for the specimens annealed at 900, 1000, and 1250 °C for 2 h after the 650 °C/2 h anneal.

annealed at 900 or 1000 °C, a considerable number of grown-in oxide precipitates can survive and further become coarsened. During this process, the fast-diffusing species of (N_2) atoms moves toward the growing oxide precipitates, which is favorable for reducing the free energy of system. It is plausible that such (N_2) atoms aggregate onto the growing oxide precipitates according to the previously reported results as mentioned above. By comparison, the (N_2) atoms diffuse much faster at 1000 °C than at 900 °C.[38] Therefore, the (N_2) atoms can be nearly exhausted by 2 h anneal at 1000 °C but not at 900 °C, which is revealed in Fig. 3. As a matter of fact, it was found in our experiment that the (N_2) atoms could also be nearly exhausted by the anneal at 900 °C for 6 h. When annealed at 1250 °C, most of the grown-in oxide precipitates are dissolved rather than coarsened because the O_i concentration (7.60×10^{17} cm^{-3}) in the NCZ silicon wafer used herein is lower than the O_i solubility (8.49×10^{17} cm^{-3}) in silicon.[39] In this context, the (N_2) atoms are hardly consumed because of nearly no growth of grown-in oxide precipitates. Namely, nearly all the (N_2) atoms are still remaining in the NCZ silicon after the 1250 °C/2 h anneal, which is manifested by the 963 cm^{-1} absorption peak nearly as strong as that of the specimen subjected to only the 650 °C/2 h anneal, as shown in Fig. 3. In combination with the results illustrated in Fig. 2, it is derived that the amount of residual N–O STDs at a given temperature is correlated with the concentration of residual (N_2) atoms, which is dependent on how the (N_2) atoms are involved into the growth of grown-in oxide precipitates.

Figure 4 shows the decrease in carrier concentration in the specimen subjected to the RTA at 900, 1000, or 1250 °C for up to 100 s following the 650 °C/2 h anneal. As in the case of Fig. 2, the decrease in carrier concentration is also indicative of the elimination of N–O STDs. As shown in Fig. 4, the carrier concentration decreases dramatically after the first 20 s RTA and then remains nearly unchanged with the extension of RTA time at each temperature. Therefore, it is derived that the N–O STDs can be significantly eliminated by the RTA for only 20 s at 900, 1000, or 1250 °C. Note in Fig. 4 that the elimination of N–O STDs by means of RTA is hardly sensitive to the temperature used herein. In combination with Fig. 2, it is found that the effect of 20 s RTA is equivalent to that of 5 min CFA in terms of the elimination of N–O STDs. Accordingly, it is speculated that most of the N–O STDs could be eliminated in the first 20 s even in the case of CFA at 900, 1000, or 1250 °C.

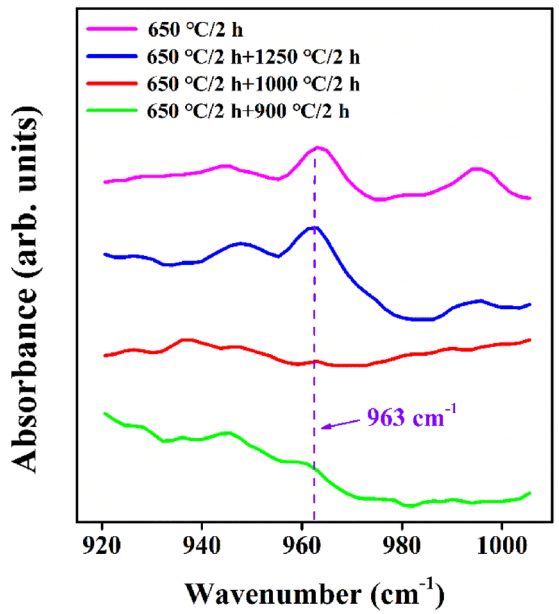

FIG. 3. RT middle-infrared FTIR spectra for the three specimens subjected to the CFA with the schemes of 650 °C/2 h + *T* °C/2 h (*T* = 900, 1000, and 1250 °C) and for the specimen only subjected to the 650 °C/2 h anneal.

Probably, the elimination of N–O STDs by means of CFA or RTA at elevated temperatures as described above could arise from the aggregation of O_i onto the N–O STDs (NO_x complexes), which leads to the electrically inactive NO_m clusters containing more oxygen atoms. Such a scenario can be expressed as

$$NO_x\ (x = 1 - 3) \overset{+O_i}{\rightarrow} NO_m\ (m > 3). \quad (1)$$

Evidently, Eq. (1) represents a kinetic process controlled by the diffusion of O_i. It is understandable that more O_i atoms will aggregate onto the N–O STDs along with the extension of anneal at a given temperature. Then, if the elimination of N–O STDs would obey Eq. (1), more N–O STDs should be eliminated by the prolonged anneal at sufficiently high temperature. In reality, the concentration of N–O STDs remains nearly unchanged with extension of annealing time in the case of the CFA at 1250 °C or the RTA at different temperatures, which can be derived from Figs. 2 or 4. Accordingly, it is believed that the elimination of N–O STDs is not a kinetic process as expressed by Eq. (1). Although the elimination of N–O STDs in the specimen subjected to the CFA at 900 or 1000 °C is increasingly significant along with the extension of annealing time, it is due to other reason as will be explained later.

B. Origin of N–O STDs

Figure 5(a) shows the optimized structure of a silicon supercell constructed with 216 Si atoms and an individual N–O STD in the

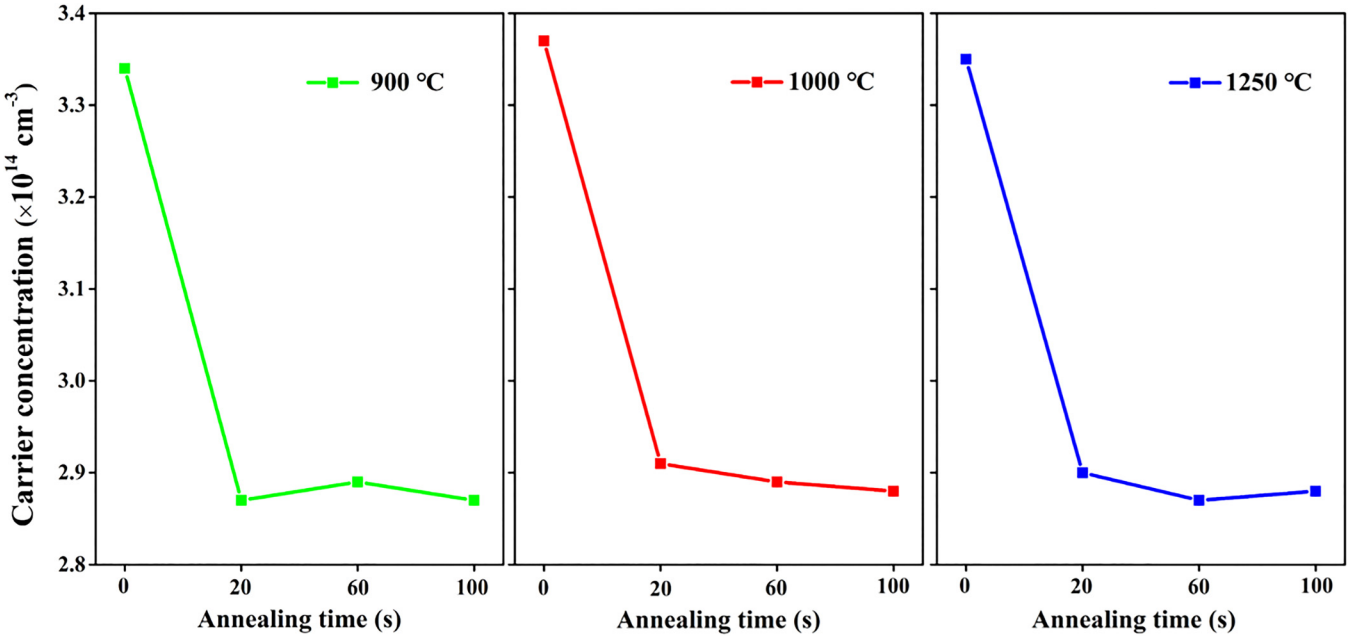

FIG. 4. The decrease in carrier concentration in the specimen subjected to the RTA at 900, 1000, or 1250 °C for up to 100 s after the 650 °C/2 h anneal.

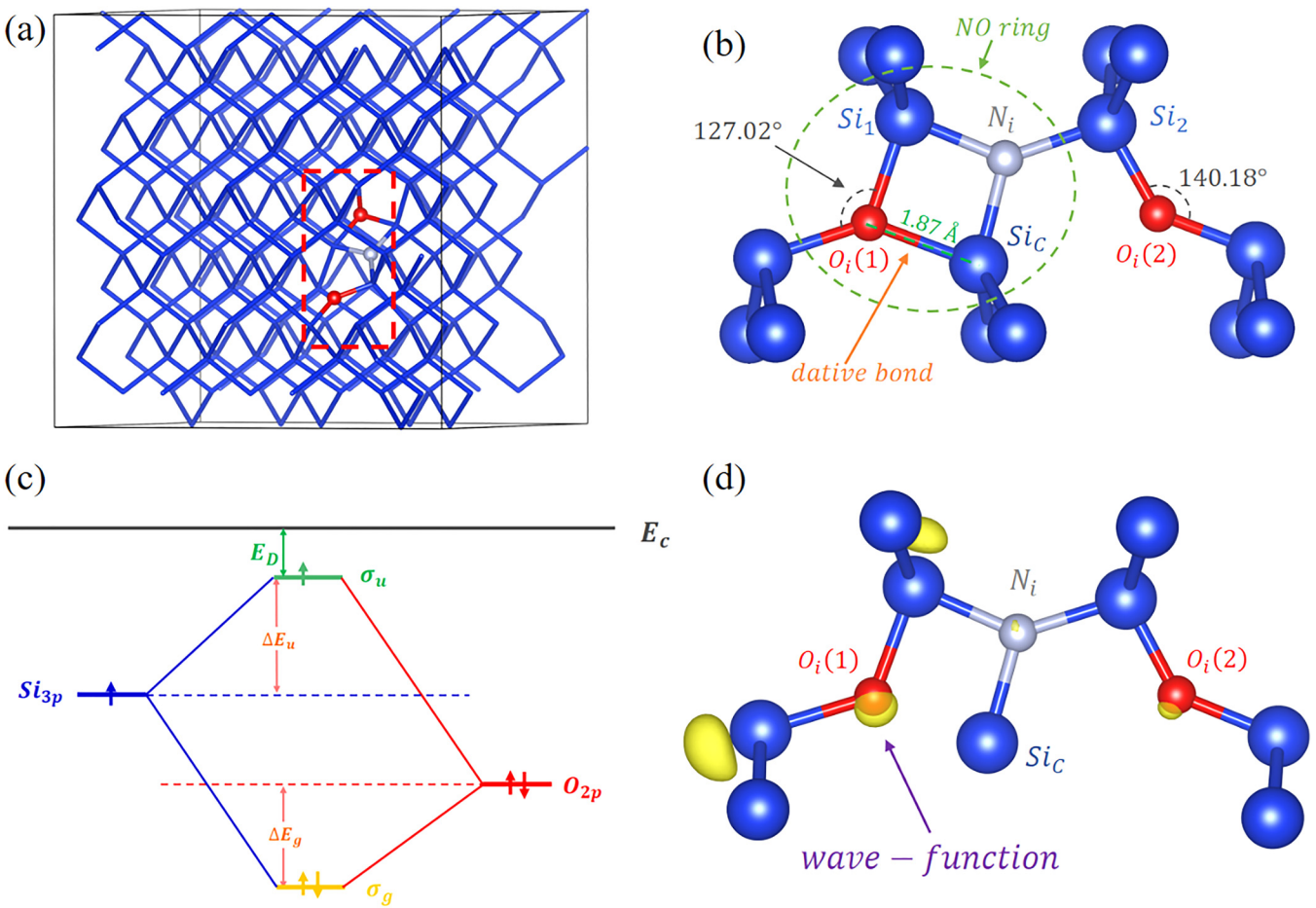

FIG. 5. (a) The optimized structure at 0 K of a silicon supercell consisting of 216 Si atoms and one N–O STD in the form of NO_2 complex. (b) The optimized configuration of the NO_2 complex. (c) The molecular orbital energy level diagram for the orbitals constructed from the overlap of Si_{3p} and O_{2p} orbitals. For reference, the conduction band edge (E_c) of silicon host is also illustrated. (d) The distribution of wave-function (in yellow) of the highest occupied orbital of the NO_2 complex.

form of an NO_2 complex at 0 K, derived from DFT calculations. The configuration of such an NO_2 complex is displayed in Fig. 5(b), which is similar to that reported by Ewels *et al.*[26] As circled in Fig. 5(b), there is a fundamental cell of "NO *ring*." Although the origin of N–O STDs has been explored in Ref. 26, herein, we attempt to combine this with molecular orbital theory to elucidate why the "NO *ring*," and furthermore the NO_2 complex becomes a STD in a succinct, easy-to-understand way based on the configuration as shown in Fig. 5(b). As a nitrogen atom is incorporated into an interstitial site of silicon lattice, it will share three covalent bonds with three adjacent Si atoms. As illustrated in Fig. 5(b), the interstitial nitrogen (N_i) atom covalently bonds with Si_1, Si_2, and Si_c atoms. If without such an N_i atom, the Si_c atom originally bonds with Si_1 and Si_2 atoms. Therefore, the incorporation of N_i atom, which breaks the Si_c–Si_1 and Si_c–Si_2 bonds, will lead to an unpaired *3p* orbital electron of the Si_c atom in the absence of a neighboring O_i atom [denoted as $O_i(1)$ in Fig. 5(b)], forming a dangling bond. In reality, the $O_i(1)$ atom is in close proximity to the Si_c atom. In this context, the *3p* orbital of Si_c atom couples with the *2p* orbital of the $O_i(1)$ atom, forming a dative bond. Note that the length (1.87 Å) of such a dative bond is much larger than that (~1.60 Å) of a conventional Si–O covalent bond in a silicon host. Figure 5(c) shows the molecular orbital energy level diagram for the orbitals constructed from the overlap of Si_{3p} and O_{2p} orbitals. Moreover, the conduction band edge (E_c) of the silicon host is also illustrated for reference. As seen, a bonding orbital (σ_g) with lower energy and an anti-bonding orbital (σ_u) with higher energy are formed. The σ_g orbital is occupied by the two electrons from the O_{2p} orbital with lower energy, while the higher energy single electron in Si_{3p} orbital enters into the σ_u orbital. In this way, the energy level of unpaired Si_{3p} electron is increased to be closer to E_c of silicon host, becoming a shallow donor level. For the NO_2 complex, the lone-pair electrons on the *2p* orbital of the $O_i(2)$ atom, which is on the right of the Si_c atom

as shown in Fig. 5(b), further pushes the σ_u level upward due to electrostatic interactions.[26] Figure 5(d) shows the wave-function of the highest occupied orbital of N–O STDs, i.e., σ_u orbital in Fig. 5(c), exhibiting the feature of delocalization, which indicates that the electron in σ_u orbital can readily become mobile in a silicon host. In view of the above analysis, it can be proposed that the elimination of N–O STDs should be essentially arisen from the destruction of the "NO *ring*."

C. MD simulation for the elimination of N–O STDs

Figure 6(a) shows the MD simulated atomic configuration for the silicon supercell in Fig. 5(a) subjected to the anneal at 1300 K for 3 ps. Compared with Fig. 5(a), it can be seen that the supercell is to a large extent distorted due to the thermal vibration. More importantly, the configuration of the "NO *ring*," and in turn the NO_2 complex as shown in Fig. 5(b) is not kept at 1300 K anymore. Instead, the arrangement of Si, N, and O atoms originally involved in the formation of the NO_2 complex as shown in Fig. 5(a) is changed as Fig. 6(b). Obviously, there is no "NO *ring*" anymore after the anneal at 1300 K, thus losing the fundamental cell of N–O STDs. Figure 6(c) demonstrates the variation of the normalized atomic spacing between N_i and $O_i(2)$, Si_C and $O_i(1)$, or Si_C and $O_i(2)$ atoms during the MD simulation process. Herein, the normalization is based on the corresponding atomic spacing illustrated in Fig. 5(b). As can be seen, the atomic spacing of Si_C–$O_i(1)$ oscillates around 0.9 times that of the original equilibrium atomic spacing, which is 1.87 Å in the optimized structure as shown Fig. 5(b). Namely, during the anneal at 1300 K, the atomic spacing of Si_C–$O_i(1)$ is around 1.68 Å, quite close to the covalent bond length of Si–O_i (~1.60 Å) in the silicon host.[40,41] In this case, the Si_C atom and the $O_i(1)$ atom are connected by a covalent bond rather than a dative bond. Instead, a dangling bond appears on the Si_1 atom, which is about 2.64 Å away from the $O_i(1)$ atom. Herein, the $3p$ orbital (Si_{3p}) of the Si_1 atom is not able to couple with the $2p$ orbital (O_{2p}) of the $O_i(1)$ atom due to such considerably large spacing between the two atoms, failing to form a dative bond to elevate the energy level of the Si_{3p} electron of the Si_1 atom. Thus, the shallow donor level cannot be generated in this context. Moreover, the normalized atomic spacing between the Si_C atom and the $O_i(2)$ atom can reach 160% and that between the N_i atom and the $O_i(2)$ atom can even exceed 200% during the MD simulation, indicating that the $O_i(2)$ atom departs from Si_C and N_i ones. In other words, the MD simulation results as mentioned above suggest that the N–O STDs can be destructed by a short period of anneal at elevated temperatures.

D. Thermodynamic analysis on N–O STDs

In a word, both the experimental and theoretical results as described above indicate that the elimination of N–O STDs at elevated temperatures is actually the decomposition of NO_x complexes into N_i and O_i atoms, which is the reverse process of forming N–O STDs. Essentially, the formation and elimination of N–O STDs are the two reversible processes, as can be expressed below,

$$NO_x \overset{k_1}{\leftrightarrow} N_i + xO_i. \tag{2}$$

According to Ref. 42, at elevated temperatures N_i atoms actually coexist with (N_2) atoms as

$$N_i \overset{k_2}{\leftrightarrow} \frac{1}{2} N_2. \tag{3}$$

Combining the above two equations, the overall reversible reaction equation can be written as

$$NO_x \overset{k_3}{\leftrightarrow} \frac{m}{2} N_2 + (1-m) N_i + xO_i. \tag{4}$$

In the above three equations, k_1, k_2, and k_3 are the equilibrium constants of the forward reactions. It can be established that $k_3 = k_1 \times k_2^m$, where m is the molar ratio of nitrogen in the form of (N_2) atoms to the total nitrogen content; thus, $m \in (0, 1)$. Moreover, m is negatively dependent on the annealing temperature. According to Eq. (4), it is known that the formation and elimination of N–O STDs will keep in dynamic equilibrium at a given temperature unless the concentrations of N_2, N_i, and O_i are changed due to specific reasons. In this way, it is understandable that there are residual N–O STDs after a short period of CFA or the RTA at 900–1250 °C. Moreover, since the elimination of N–O STDs is a temperature-controlled decomposition process, most of the N–O STDs can be annihilated in a short period of time at sufficiently high temperatures, which can be seen in Figs. 2 and 4.

It is well documented that the generation of N–O STDs is significant at low temperatures such as 650 °C.[11,12] On the other hand, the elimination of N–O STDs is predominant at elevated temperatures such as 900 and 1000 °C,[28] which has been again verified in this work. The behavior of N–O STDs, dependent on the temperature as mentioned above, can be understood from the thermodynamic point of view based on Eq. (2), which is described as follows.

Addressing Eq. (2), we suppose that the enthalpies before and after the decomposition of NO_x complexes are H_1 and H_2, respectively. Thus, the enthalpy change due to the decomposition of NO_x complexes is

$$\Delta H = H_2 - H_1. \tag{5}$$

When the reaction (annealing) temperature is T_1, the enthalpy change can be expressed as

$$\Delta H(T_1) = \Delta H(0\ \mathrm{K}) + \int_0^{T_1} \Delta C(T)\, dT, \tag{6}$$

where $\Delta H(0\ \mathrm{K})$ is the enthalpy change at 0 K and $\Delta C(T)$ is the change in heat capacity due to the decomposition of NO_x complexes. Figure 7(a) shows the curve of $\Delta C(T)$, which is derived from the DFT calculations. As can be seen, ΔC is always positive in the temperature range of 0–1500 K. Moreover, the entropy change due to the decomposition of NO_x complexes at T_1 is

$$\Delta S(T_1) = \int_0^{T_1} \frac{\Delta C(T)}{T} dT. \tag{7}$$

Then, the Gibbs free energy change of the decomposition of NO_x

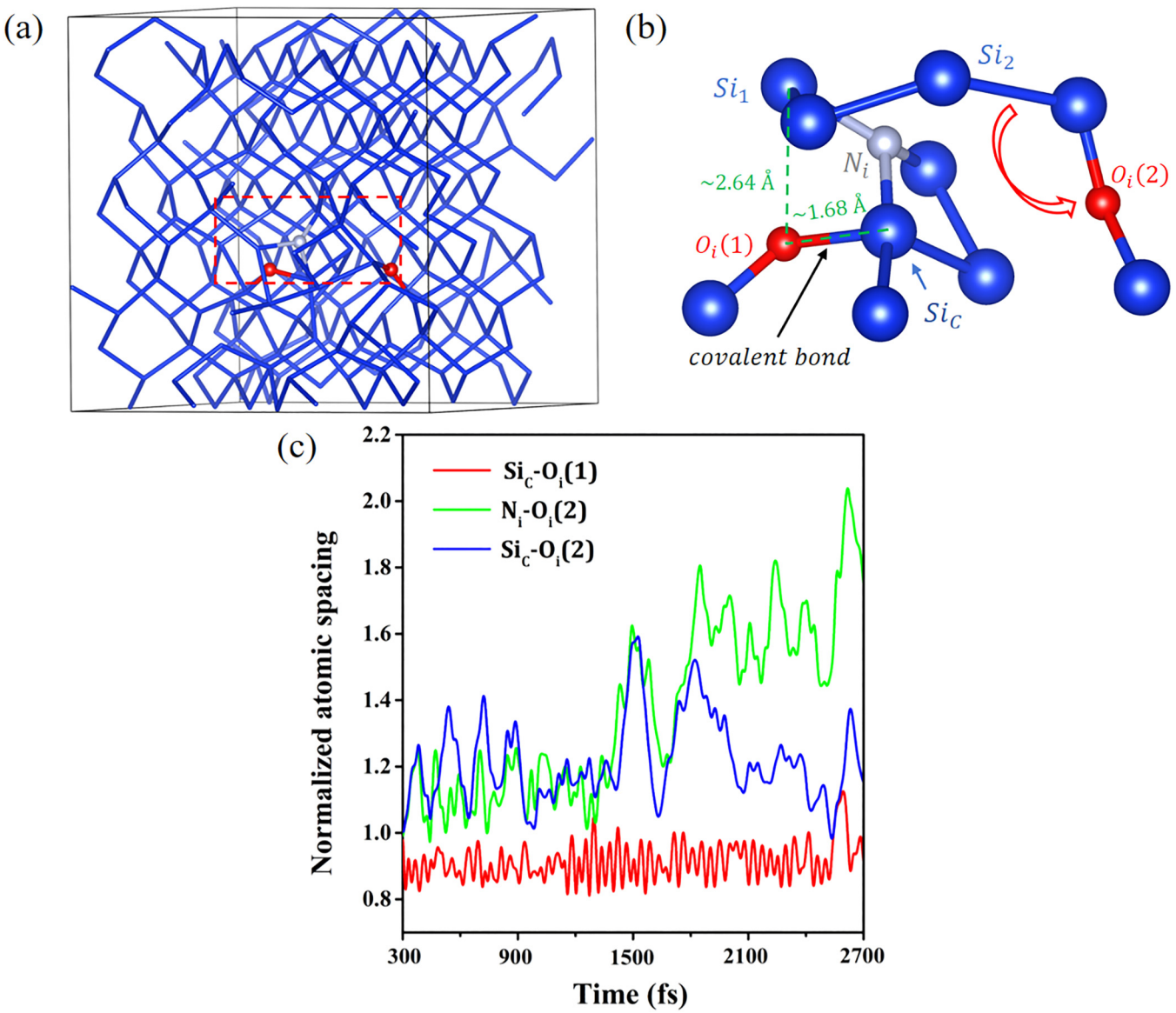

FIG. 6. (a) MD simulated atomic configuration for the silicon supercell in Fig. 5(a) subjected to the anneal 1300 K for 3 ps. (b) The arrangement of Si, N, and O atoms originally involved in the formation of NO_2 complex as shown in Fig. 5(a) after the anneal 1300 K for 3 ps. (c) The variation of normalized atomic spacing between N_i and $O_i(2)$, Si_C and $O_i(1)$, or Si_C and $O_i(2)$ atoms during the MD simulation at 1300 K. Note that the normalization is based on the corresponding atomic spacing illustrated in Fig. 5(b).

complexes is

$$\Delta G(T_1) = \Delta H(T_1) - T_1 \times \Delta S(T_1). \tag{8}$$

Combining Eq. (6) with Eq. (8), we have

$$\Delta G(T_1) = \Delta H(0K) + \int_0^{T_1} \Delta C(T) \times \left(1 - \frac{T_1}{T}\right) dT. \tag{9}$$

Since T_1 is the upper limit of the integral term in Eq. (9), which is always higher than T, we have

$$\int_0^{T_1} \Delta C(T) \times \left(1 - \frac{T_1}{T}\right) dT < 0. \tag{10}$$

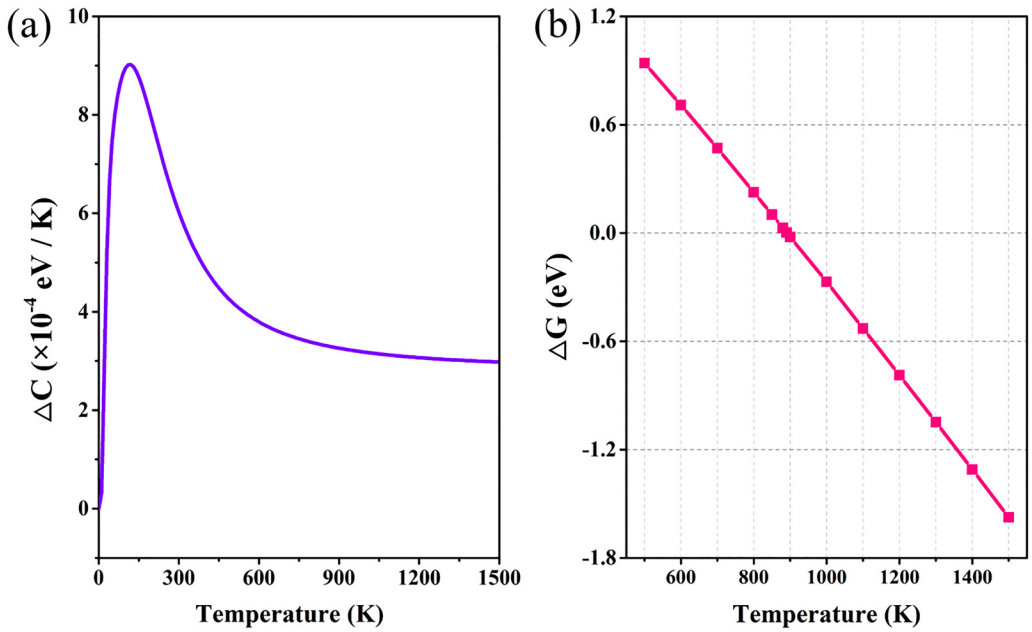

FIG. 7. (a) The change in heat capacity (ΔC) due to the decomposition of NO_x complexes as a function of temperature. (b) The change in Gibbs free energy (ΔG) as a function of annealing temperature for the reaction expressed as Eq. (2), calculated according to Eq. (9).

To ensure the decomposition of NO_x complexes, we should have

$$\Delta G(T_1) < 0. \tag{11}$$

Then,

$$\int_0^{T_1} \Delta C(T) \times \left(1 - \frac{T_1}{T}\right) dT < -\Delta H(0\ \mathrm{K}). \tag{12}$$

Based on the DFT calculations, it is obtained that $\Delta H(0\ \mathrm{K}) = 1.77$ eV. Therefore, T_1 should be sufficiently large to satisfy the conditions as described in the above inequality (12). Namely, as the reaction temperature is high enough, the change of free energy (ΔG) for Eq. (2) in the forward direction is negative, meaning that the decomposition of NO_x complexes and, therefore, the elimination of N–O STDs is energetically favorable. Conversely, as the reaction temperature is insufficiently high, the inequality (12) cannot be satisfied. In this context, the reaction in Eq. (2) will proceed in the backward direction, resulting in the generation of N–O STDs. So far, based on the above thermodynamic analysis, it can be qualitatively understood why the N–O STDs are significantly generated at relatively low temperature such as 650 °C, whereas they are substantially eliminated at 900 °C and above. Actually, according to Eq. (9), the temperature dependence of ΔG for the reaction expressed as Eq. (2) can be calculated, which is shown in Fig. 7(b). Therein, the crossover temperature according to $\Delta G = 0$ is ~900 K. Nevertheless, in order to enable the forward reaction in Eq. (2) to proceed remarkably, ΔG should be much smaller than zero. As can be seen from Fig. 7(b), ΔG is of considerably large negative value at 900 °C (~1173 K) and above, indicating that the decomposition of NO_x complexes, i.e., the elimination of N–O STDs is quite energetically favorable in the aforementioned temperature regime.

As can be derived from Fig. 2, the concentration of residual N–O STDs remains nearly constant with the extension of annealing time at 1250 °C, while it decreases progressively with the prolonged anneal at 900 or 1000 °C. Besides, as can be derived from Fig. 4, the concentration of residual N–O STDs hardly changes with the extension of RTA time at different temperatures. Such phenomena can also be comprehended from the standpoint of thermodynamics using the Eq. (4), which is described as follows.

When the forward and backward reactions in Eq. (4) reach equilibrium at a given temperature, the concentration of residual N–O STDs ($[NO_x]$) can be expressed as

$$[NO_x] = \frac{1}{k_3} \times [N_2]^{\frac{m}{2}} \times [N_i]^{1-m} \times [O_i]^x, \tag{13}$$

where $[N_2]$, $[N_i]$, and $[O_i]$ are the concentrations of (N_2) atoms, N_i, and O_i, respectively. It is considered that the nitrogen impurity in silicon is mainly in the forms of (N_2) atoms and N_i at elevated temperatures, since the concentration of N–O complexes is generally at least one order of magnitude lower than that of (N_2) atoms or N_i. Denoting the total nitrogen concentration as [N], then $[N_2] = \frac{m}{2} \times [N]$ and $[N_i] = [N] - 2[N_2] = (1 - m) \times [N]$. Thus,

$$[N_i] = \frac{2\ (1-m)}{m} \times [N_2]. \tag{14}$$

Combining Eq. (14) with Eq. (13), $[NO_x]$ can be expressed as

$$[NO_x] = \frac{1}{k_1 \times k_2^m} \times \left(2 \times \frac{1-m}{m}\right)^{1-m} \times [N_2]^{1-\frac{m}{2}} \times [O_i]^x. \quad (15)$$

Since $0 < m < 1$ and $1 \leq \times \leq 3$, the concentration of N–O STDs ($[NO_x]$) is positively correlated to $[N_2]$ and $[O_i]$ according to Eq. (15). In the case of CFA with the annealing time up to only 2 h, $[O_i]$ can be regarded to be nearly constant, while $[N_2]$ is decreased during the CFA at 900 or 1000 °C, due to the aggregation of (N_2) atoms onto the growing oxide precipitates as mentioned above, and is nearly unchanged during the CFA at 1250 °C, as shown in Fig. 3. Consequently, $[NO_x]$ decreases progressively with the extension of annealing time at 900 or 1000 °C, while is nearly constant during the prolonged CFA at 1250 °C, as can be derived from Fig. 2(a). In the case of RTA, $[N_2]$ and $[O_i]$ are hardly changed with the extension of annealing time, thus leading to nearly unchanged $[NO_x]$, as can be derived from Fig. 4.

Last but not least, it can be derived from Figs. 2(a) or 4 that the concentration of residual N–O STDs after 5 min CFA or 20 s RTA is nearly independent on the annealing temperature. This result can be qualitatively explained as follows.

Based on Eqs. (2)–(4), it is derived that

$$[NO_x] = \frac{1}{k_1} \times (1-m) \times [N] \times [O_i]^x, \quad (16)$$

where m becomes smaller as the temperature is raised.

According to van't Hoff equation,[43] we have

$$\frac{d \ln k_1}{d T} = \frac{\Delta H}{R \times T^2}, \quad (17)$$

where $\Delta H > 0$, as can be known from Eq. (6). Therefore, k_1 becomes larger as the temperature is raised. Consequently, the value of the term of $\frac{1}{k_1} \times (1-m)$ in Eq. (16) may change little as the temperature is raised because k_1 is increased while m is decreased, as mentioned above. Moreover, $[N]$ and $[O_i]$ are little changed after the brief CFA or the RTA at different temperatures. Then, according to Eq. (16), we can understand that the concentration of residual N–O STDs ($[NO_x]$) changes little after a short period of CFA or the RTA at different temperatures ranging from 900 to 1250 °C.

V. CONCLUSION

We have systematically addressed the issue of the elimination of N–O STDs in NCZ silicon. Experimentally, the elimination of N–O STDs has been investigated by means of CFA and RTA at elevated temperatures ranging from 900 to 1250 °C. In the case of CFA, the N–O STDs are remarkably eliminated by the first 5 min anneal at different temperatures and then they are progressively eliminated at 900 or 1000 °C with the extension of annealing time up to 2 h, while they are hardly eliminated by the prolonged anneal at 1250 °C, which is somewhat out of expectation. It is found that there are much more (N_2) atoms remaining after the 1250 °C/2 h anneal than after the 900 or 1000 °C/2 h counterpart, which is responsible for the more residual N–O STDs after the 1250 °C/2 h anneal. It is speculated that the loss of (N_2) atoms during the CFA at 900 or 1000 °C is due to the (N_2) atoms that are involved into the growth of grown-in oxide precipitates. In the case of RTA, the N–O STDs are significantly eliminated in the first 20 s and then keep nearly the same amount with the extension of annealing time. Moreover, the concentrations of residual N–O STDs after the RTA at different temperatures are nearly the same. The aforementioned results indicate that the N–O STDs in NCZ silicon can be mostly eliminated by a short period of anneal at elevated temperatures, which is actually solid evidence for the viewpoint that the elimination of N–O STDs is ascribed to the decomposition of NO_x complexes. Theoretically, we have elucidated the origin of N–O STDs through combining the DFT calculations with the molecular orbital theory. On this basis, it is understood that the elimination of N–O STDs is essentially ascribed to the destruction of the core "NO *ring*," which has been further confirmed by the MD simulation at 1300 K. In view of the experimental and theoretical results as mentioned above, we have made a comprehensive thermodynamic analysis on the behavior of N–O STDs in NCZ silicon to account for the phenomena revealed in the experiments. We believe that this work has gained an in-depth understanding of N–O STDs in NCZ silicon.

ACKNOWLEDGMENTS

The author would like to acknowledge the financial support from the Natural Science Foundation of China (Grant Nos. 61674126, 51532007, and 61721005).

DATA AVAILABILITY

The data that support the findings of this study are available from the corresponding authors upon reasonable request.

REFERENCES

[1]K. Sumino, I. Yonenaga, M. Imai, and T. Abe, J. Appl. Phys. **54**, 5016–5020 (1983).
[2]J. D. Murphy, C. R. Alpass, A. Giannattasio, S. Senkader, R. J. Falster, and P. R. Wilshaw, Nucl. Instrum. Methods Phys. Res. Sect. B **253**, 113–117 (2006).
[3]X. Yu, D. Yang, X. Ma, J. Yang, L. Li, and D. Que, J. Appl. Phys. **92**, 188–194 (2002).
[4]A. Karoui, F. S. Karoui, G. A. Rozgonyi, and D. Yang, J. Appl. Phys. **96**, 3255–3263 (2004).
[5]A. Karoui and G. A. Rozgonyi, J. Appl. Phys. **96**, 3264–3271 (2004).
[6]K. Nakai, Y. Inoue, H. Yokota, A. Ikari, J. Takahashi, A. Tachikawa, K. Kitahara, Y. Ohta, and W. Ohashi, J. Appl. Phys. **89**, 4301–4309 (2001).
[7]F. Shimura and R. S. Hockett, Appl. Phys. Lett. **48**, 224–226 (1986).
[8]Q. Sun, K. H. Yao, H. C. Gatos, and J. Lagowski, J. Appl. Phys. **71**, 3760–3765 (1992).
[9]K. Aihara, H. Takeno, Y. Hayamizu, M. Tamatsuka, and T. Masui, J. Appl. Phys. **88**, 3705–3707 (2000).
[10]M. Suezawa, K. Sumino, H. Harada, and T. Abe, Jpn. J. Appl. Phys. **25**, L859–L861 (1986).
[11]M. Suezawa, K. Sumino, H. Harada, and T. Abe, Jpn. J. Appl. Phys. **27**, 62–67 (1988).
[12]A. Hara, T. Fukuda, T. Miyabo, and I. Hirai, Appl. Phys. Lett. **54**, 626–628 (1989).

[13]C. S. Chen, C. F. Li, H. J. Ye, S. C. Shen, and D. Yang, J. Appl. Phys. **76**, 3347–3350 (1994).
[14]D. Yang, D. Que, and K. Sumino, J. Appl. Phys. **77**, 943–944 (1995).
[15]R. C. Newman, J. H. Tucker, N. G. Semaltianos, E. C. Lightowlers, T. Gregorkiewicz, I. S. Zevenbergen, and C. A. J. Ammerlaan, Phys. Rev. B **54**, R6803–R6806 (1996).
[16]H. C. Alt and H. E. Wagner, Phys. Rev. B **82**, 115203 (2010).
[17]P. Wagner, R. Oeder, and W. Zulehner, Appl. Phys. A **46**, 73–76 (1988).
[18]V. V. Voronkov, M. Porrini, P. Collareta, M. G. Pretto, R. Scala, R. Falster, G. I. Voronkova, A. V. Batunina, V. N. Golovina, L. V. Arapkina, A. S. Guliaeva, and M. G. Milvidski, J. Appl. Phys. **89**, 4289–4293 (2001).
[19]R. Jones, S. Oberg, F. B. Rasmussen, and B. B. Nielsen, Phys. Rev. Lett. **72**, 1882–1885 (1994).
[20]H. Sawada and K. Kawakami, Phys. Rev. B **62**, 1851–1858 (2000).
[21]J. P. Goss, I. Hahn, R. Jones, P. R. Briddon, and S. Öberg, Phys. Rev. B **67**, 045206 (2003).
[22]H. C. Alt, H. E. Wagner, W. V. Ammon, F. Bittersberger, A. Huber, and L. Koester, Physica B **401**, 130–133 (2007).
[23]H. E. Wagner, H. C. Alt, W. v. Ammon, F. Bittersberger, A. Huber, and L. Koester, Appl. Phys. Lett. **91**, 152102 (2007).
[24]A. Gali, J. Miro, P. Deak, C. P. Ewels, and R. Jones, J. Phys.: Condens. Mater. **8**, 7711–7722 (1996).
[25]N. Fujita, R. Jones, S. Oberg, and P. R. Briddon, Physica B **401**, 159–162 (2007).
[26]C. P. Ewels, R. Jones, S. Oberg, J. Miro, and P. Deak, Phys. Rev. Lett. **77**, 865–868 (1996).
[27]D. Yang, R. Fan, L. Li, D. Que, and K. Sumino, J. Appl. Phys. **80**, 1493–1498 (1996).
[28]D. Yang, R. Fan, L. Li, D. Que, and K. Sumino, Appl. Phys. Lett. **68**, 487–489 (1996).
[29]H. C. Alt and H. E. Wagner, J. Appl. Phys. **106**, 103511 (2009).
[30]J. Hafner, J. Comput. Chem. **29**, 2044–2078 (2008).
[31]G. Kresse and J. Furthmuller, Phys. Rev. B **54**, 11169–11186 (1996).
[32]G. Kresse and J. Furthmuller, Comput. Mater. Sci. **6**, 15–50 (1996).
[33]J. P. Perdew, K. Burke, and M. Ernzerhof, Phys. Rev. Lett. **77**, 3865–3868 (1996).
[34]B. Delley, J. Chem. Phys. **113**, 7756–7764 (2000).
[35]A. Kvit, A. Karoui, G. Duscher, and G. A. Rozgonyi, Appl. Phys. Lett. **84**, 1889–1891 (2004).
[36]L. S. Adam, M. E. Law, O. Dokumaci, Y. Haddara, C. Murthy, H. Park, S. Hegde, D. Chidambarrao, S. Mollis, T. Domenicucci, C. Dziobkowski, K. Jones, P. Wong, R. Young, and R. Srinivasan, MRS Proc. **568**, 277–281 (1999).
[37]L. Shaik Adam, M. E. Law, K. S. Jones, O. Dokumaci, C. S. Murthy, and S. Hegde, J. Appl. Phys. **87**, 2282–2284 (2000).
[38]T. Itoh and T. Abe, Appl. Phys. Lett. **53**, 39–41 (1988).
[39]A. Borghesi, B. Pivac, A. Sassella, and A. Stella, J. Appl. Phys. **77**, 4169–4244 (1995).
[40]R. Jones, A. Umerski, and S. Oberg, Phys. Rev. B **45**, 11321–11323 (1992).
[41]C. P. Ewels, R. Jones, and S. Öberg, Mater. Sci. Forum **196–201**, 1297–1302 (1995).
[42]V. V. Voronkov and R. J. Falster, Solid State Phenom. **95–96**, 83–92 (2003).
[43]P. W. Atkins, J. C. D. Paula, and J. Keeler, *Atkins' PHYSICAL Chemistry* (Oxford University Press, 2018), p. 246.